Wind turbine drive-train condition monitoring through tower vibrations measurement and processing

Wind turbine drive-train condition monitoring through tower vibrations measurement and processing

D. Astolfi [1], **A.P. Daga** [2], **F. Natili** [1], **F. Castellani** [1], **L. Garibaldi** [2]
[1] University of Perugia, Department of Engineering
Via G. Duranti 93, 06125, Perugia, Italy

[2] Politecnico di Torino, Department of Mechanical and Aerospace Engineering
Corso Duca degli Abruzzi 24, 10129, Torino, Italy,
e-mail: **davide.astolfi@unipg.it**

Abstract
Robust condition monitoring of geared wind turbine drive-train is in general very challenging because of the complex non-stationary operation conditions to which the machine is subjected. Nevertheless, this issue is particularly important because gearbox damages account for at least the 20% of wind turbines unavailability time. In this work, a new method for wind turbine drive-train condition monitoring is proposed: the general idea is that vibrations are measured at the tower, instead that at the drive-train. The strength point of this approach is that measurements can be easily performed in industrial plants without security issues and without interrupting the normal operation. The drawback is that extracting knowledge about the drive-train from tower vibration data is challenging: in this work, the main idea for circumventing this issue has been to measure vibrations simultaneously at the highest possible number of wind turbines in the wind farm of interest. The general idea for processing the data is selecting one wind turbine as target for the validation and the other wind turbines as references for training and testing. The data are analysed in the time domain and the most common statistical features (root mean square, peak, crest factor, skewness, kurtosis) are computed on independent chunks of the vibration time series. The resulting data set in the feature space therefore reduces to a matrix, from which the rows corresponding to the target wind turbine, if there is a damage, should be highlighted as statistically distinguishable with respect to the rest of the matrix. The application of this algorithm is justified by univariate statistical tests on the selected time-domain features and by a visual inspection of the data set via Principal Component Analysis. Finally, a novelty index based on the Mahalanobis distance is used to detect the possible anomalous conditions at the target wind turbine. The present work is based on field measurement campaigns, performed by the authors at the wind farms owned by the Renvico company during years 2018 and 2019 and 2020: this has allowed testing the data processing methods on several damage test cases of different severity and the main result is that it is possible to successfully individuate damaged wind turbines.

1 Introduction

The diagnosis of gears and bearings faults of gearbox-based systems [1] is particularly challenging, especially if the operation conditions are non-stationary.

This is true in particular for modern horizontal-axis wind turbine technology: wind turbines operate in field under non-stationary conditions that can likely be extreme and are affected by the ambient turbulence. In the recent review [2] about wind turbine gearbox condition monitoring through vibration analysis, the study in [3] is cited, basing on which gearbox failures account for the order of 25% of all the wind turbine failures; furthermore, the average downtime for this kind of failures is particularly high [4]. In [5], it is estimated that bearings cause around 70% of gearbox downtime and 21–70% of generator downtime depending on wind turbine size: 21% on small generators (rated power lower than 1 MW), 70% on medium generators (rated

power between 1 MW and 2 MW) and 50% on large generators (rated power higher than 2 MW).

On these grounds, it is evident that an efficient vibration-based wind turbine drive-train condition monitoring passes through the separation of the faulty signatures from the masking signals, due to the other rolling elements like the gears or the shafts and this is a complex objective because wind turbines are subjected to non-stationary conditions. A powerful methodology is based on the fact that the signatures due to gears and shafts are deterministic and fault signatures are stochastic and can be treated as cyclo-stationary [6] around their fundamental period. The downside of this kind of analysis is that the angular speed of the rotor must be measured with high sampling rate and therefore its application to wind turbines operating in field is far from obvious: for this reason, several studies deal with numerical simulations [7] and laboratory test rig measurements [8].

Real world data are analyzed for example in [9], where Signal Intensity Estimator is employed for tackling not only high-dimensionality field data but also very extremely modulated data; furthermore, visual inspection (through Principal Component Analysis) of statistical features extracted from the data sets of interest result being particularly useful for the prognostic analysis.

Basing on these considerations, the general idea of the present study is inquiring if it is possible to detect wind turbine drive-train damages by processing appropriately vibration measurements collected at the tower. The rationale for this purpose is that tower vibrations have the great pro that they can be collected without impacting on wind turbine operation and therefore could in perspective be used as unsupervised diagnostic tool on vasts wind turbine portfolios; the drawback is that this kind of measurements must be treated like a black box in lack of the transfer function from the component of interest to the tower. The study in [10] provides meaningful indications of the fact that it is possible diagnosing wind turbine drive-train faults through tower vibration measurements: this kind of measurements is processed through Empirical Mode Decomposition and the outcomes are correlated with the vibration signals acquired directly from the target damaged generator bearings.

The objective of this study is renouncing to the crosscheck against vibration measurements collected at the damaged subcomponent because the perspective is contributing to a framework for unsupervised condition monitoring: therefore, only tower vibration measurements collected by the authors are employed for the present study. The keystone for reliably detecting anomalies is comparing wind turbines in the same wind farm: measurements are acquired simultaneously or nearly-simultaneously at the highest possible number of wind turbines.

Measurements have been collected at a wind farm sited in Italy, owned by the Renvico company, featuring six 2 MW wind turbines. Five wind turbines have been selected for this study: three reference healthy ones and two target ones. The former target wind turbine is damaged at the high-speed shaft bearing (as independently indicated by oil particle counting analysis), the latter target wind turbine had a planetary shaft bearing damage and the bearing of interest was substituted some weeks before the measurement campaign was conducted. It should be noticed that further measurement campaigns and further test case studies had to be conducted in the early months of 2020 but it resulted impossible due to the COVID-19 outbreak and therefore the present study has overlaps with [11].

If the methods proposed in this work are reliable, it should be possible to distinguish the damaged target wind turbine with respect to the reference healthy ones, while the recovered wind turbine should be indistinguishable with respect to the reference ones. In this study, it is shown that this is indeed the case. Summarizing, the post-processing algorithm proceeds as follows: vibration measurements are analyzed in the time domain through a multivariate Novelty Detection algorithm based on the analysis of simple statistical features; the application of this algorithm is supported on the ground of visual inspection of the statistical features data set through Principal Component Analysis. Finally, a novelty index based on the Mahalanobis distance is used to distinguish the target from the reference wind turbines.

The structure of the manuscript is therefore the following: in Section 2, the test case and the measurements are described; Section 3 is devoted to the methods; in Section 4 the results are collected and discussed; finally, in Section 5 conclusions are drawn and further directions of this study are indicated.

2 Test case description

The wind farm is composed of six 2 MW wind turbines and it is sited in southern Italy. The layout of the wind farm is reported in Figure 1: the damaged wind turbine (WTG03) is indicated in red, the healthy reference wind turbines (WTG02, WTG04, WTG05) are indicated in green and the recovered wind turbine (WTG06) is indicated in blue. The damage at WTG03 regards the high speed shaft bearing, the recovered damage at WTG06 regarded a planetary bearing. WTG03 has been independently diagnosed on the basis of oil particle counting and it has operated for four months from detection to intervention. When the measurements for this work have been conducted, WTG03 was operating normally.

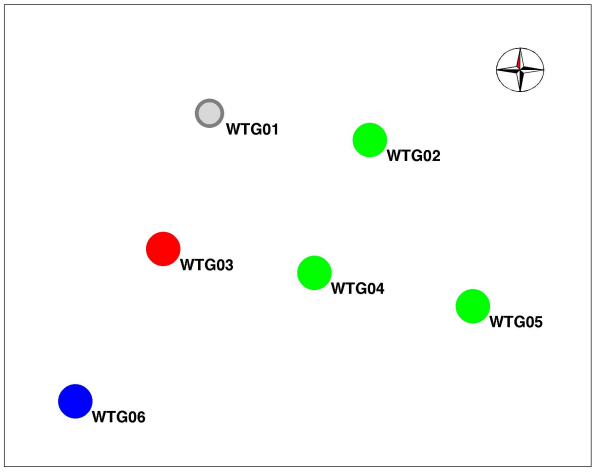

Figure 1: The layout of the wind farm. The healthy wind turbines are indicated in green, the damaged in red and the recovered in blue.

The measurement procedure is the following: accelerometers have been employed inside the tower of the wind turbine, measuring the longitudinal (x-axis) and transversal (y-axis) vibrations at a a height of the order of two meters with respect to the tower base. A sketch is reported in Figure 2. Each acquisition therefore consists of 2 channels and these are sampled at 12.8 kHz for at least 2 minutes.

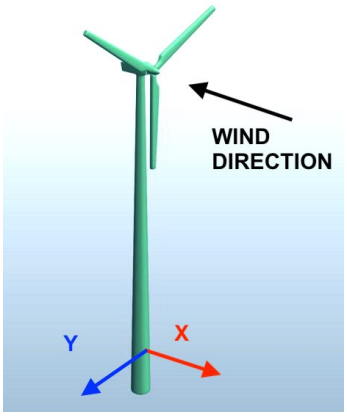

Figure 2: Definition of the reference frame for the longitudinal and the transversal directions.

The vibration time series have been organized as indicated in Table 1. It is important to notice that acquisitions have been performed within 3 hours, but there are always two contemporary acquisitions (one at a

reference wind turbines and one at the target ones), so that the risk that operational or environmental effects could be confounded for damage is reduced.

Table 1: The time series selection

TS number	Wind turbine	Wind turbine status	Acquisition time	Use	Generator rpm
1	WTG02	healthy	14:15	reference - calibration	1362
2	WTG04	healthy	14:55	reference - calibration	1199
3	WTG05	healthy	15:25	reference - calibration	1185
4	WTG02	healthy	14:25	reference - validation	1242
5	WTG04	healthy	15:05	reference - validation	1376
6	WTG05	healthy	15:35	reference - validation	1083
7	WTG06	repaired	13:00	target - validation	1694
8	WTG06	repaired	13:10	target - validation	1584
9	WTG06	repaired	13:20	target - validation	1537
10	WTG03	damaged	13:00	target - validation	1585
11	WTG03	damaged	13:10	target - validation	1468
12	WTG03	damaged	13:20	target - validation	1579
13	WTG03	damaged	14:15	target - validation	1338
14	WTG03	damaged	14:25	target - validation	1399
15	WTG03	damaged	14:55	target - validation	1333
16	WTG03	damaged	15:05	target - validation	1365
17	WTG03	damaged	15:25	target - validation	1274
18	WTG03	damaged	15:35	target - validation	1207

3 Methods

The data pre-processing proposed in this work consists of three steps:

1. a pre-treatment of the single accelerometric tracks to remove possible non-physical trends (due, for example, to disturbances);
2. the extraction of the selected statistical features;
3. a multivariate anomaly cleaning, in order to remove from the analysis the chunks of the signal that likely describe the wind turbine in adaptation to a change of the work condition.

The method for damage detection is divided in three sub-analyses [12]:

1. at first the goodness of the selected features and of the pre-processing is assessed univariately. This is performed as a univariate test of hypothesis exploiting the ANOVA (Univariate Analysis of Variance) to investigate the damage detection ability of the single features extracted from the two different channels.
2. Then, in order to visualize the multivariate dataset, a Principal Component Analysis is performed.
3. Finally, an unsupervised damage detection implemented in terms of multivariate Novelty Detection is used to detect the damaged wind turbine distinguishing from the other machines.

A scheme of the work flow is reported in Figure 3.

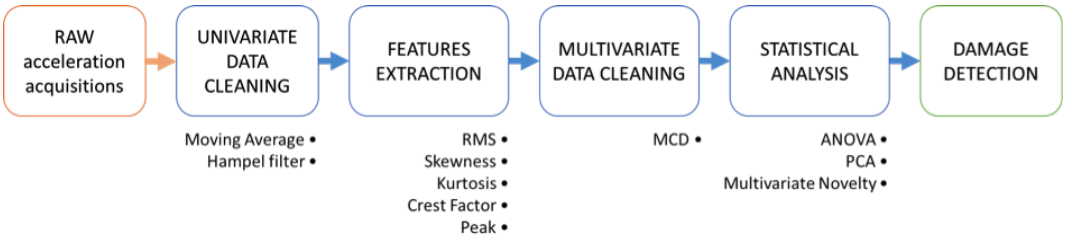

Figure 3: Block diagram of the data analysis procedure.

3.1 Data pre-processing

Some available acceleration signals have non-physical trends, probably due to the strong electromagnetic fields which can interest the area around wind farm. In signal processing, it is very common to deal with trends by considering them as the low-frequency content of the signal, which can be then divided into a long-term contribution (i.e. the trend), and a short term (high frequency) contribution. Hence, a trend can be highlighted by low-pass filtering the original signal to remove the high-frequency fluctuations: in the present study, the moving average filter [13] with a cut-off of the order of 500 Hz has been employed.

Furthermore, some abnormal spikes can still be found in the residual signal. In order to compensate also for this effect, a Hampel filter is used. The Hampel filter is an on-line two steps procedure meant to identify univariate local outliers and substitute such samples with more plausible values. To ensure robustness, the local outliers are not identified through the usual 3σ rule, but using the median and the Median Absolute Deviation (MAD) [14, 15]. If a sample from the windowed signal s_w (i.e., a chunk of the signal in the $\pm MM$ samples range) falls out of the confidence interval of

$$|s_w - median(s_w)| \leq 3 \cdot 1.4826 MAD \tag{1}$$

it is considered an outlier and is removed and substituted with the median value $\mathrm{median(s_w)}$. In this work, a window of $MM = \pm 22$ samples was used.

The final result of data pre-processing in depicted in Figures 4 and 5. Figure 4 deals with a sample time series and Figure 5 deals with the zoom on a time series excerpt. The upper plots in Figure 4 and 5 represent the raw data and the data trend (filtered with the moving average), the lower plots represent the data trend and the data trend removed of the outliers (through the Hampel filter).

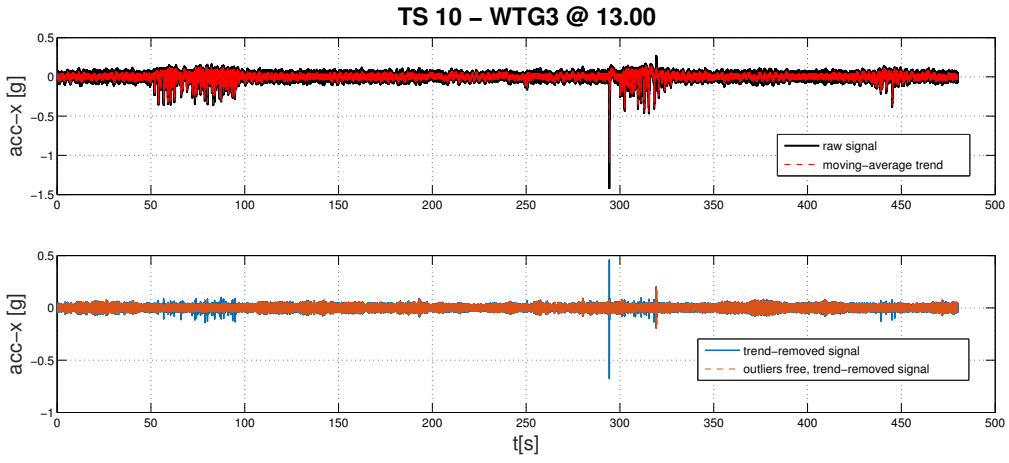

Figure 4: A sample time series of the raw and processed signal.

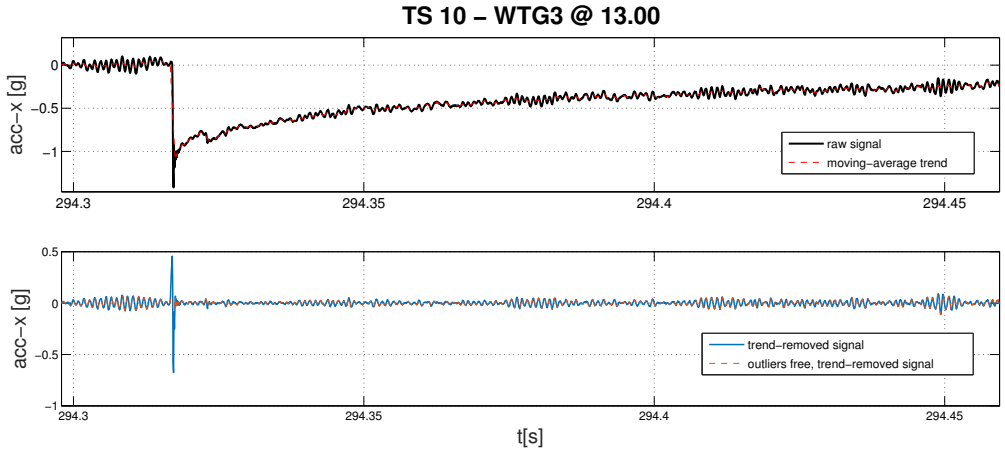

Figure 5: Zoom on a sample time series of the raw and processed signal.

3.2 Features extraction

The following statistical features have been selected for this study:

1. Root Mean Square;
2. Skewness;
3. Kurtosis;
4. Peak;
5. Crest Factor.

To guarantee the reliability of the method, many measurement points are necessary [16]. The above features have therefore been extracted on independent (no overlap) excerpts of the original signals: each acquisition is divided in 100 sub-parts on which the five features are computed. Doing this, one obtains a features matrix X where the number of columns is $n = 10$ and it is given by the product of the number of channels (2) times the number of computed features (5); the number of rows is $d = 1800$ and it corresponds to number of chunks extracted from the 18 acquisitions of Table 1 placed consecutively.

3.3 Multivariate data cleaning

An automatic routine is here proposed for removing the data-points in the 10-dimensional ($d = 10$) feature space (5 features, 2 channels) which are multivariate outliers with respect to the sample of 100 observations corresponding to that particular acquisition. The routine is based on the multi-dimensional generalization of the 3σ rule.

This can be easily implemented through the Mahalanobis distance, which corresponds to the standardized distance of a point from the centroid $\left(\bar{X}\right)$ of the ellipsoid defined by the covariance matrix $\boldsymbol{S} = \frac{1}{N}\left(\boldsymbol{X} - \bar{\boldsymbol{X}}\right)\left(\boldsymbol{X} - \bar{\boldsymbol{X}}\right)^T$ The Mahalanobis distance MD is defined as (Equation 2):

$$MD = \sqrt{\left(\boldsymbol{X} - \bar{\boldsymbol{X}}\right)\boldsymbol{S}^{-1}\left(\boldsymbol{X} - \bar{\boldsymbol{X}}\right)}, \tag{2}$$

so that, if the estimates $\bar{\boldsymbol{X}}$ and $\boldsymbol{S}$ can be confused with the true values and $\boldsymbol{X}$ is assumed normal, the simple confidence interval based on the chi-squared (χ^2) critical value holds (Equation 3):

$$MD < \sqrt{\chi^2_{d;0.997}}. \tag{3}$$

If the assumption of a χ^2 distribution for the MD does not hold, a simple but effective method for getting robust estimates of $\bar{\boldsymbol{X}}$ and $\boldsymbol{S}$ is thorough the Minimum Covariance Determinant (MCD) [17].

3.4 Hypothesis test

The ANOVA (univariate Analysis Of Variance) is a statistical method based on the analysis of variance and it is employed to test the null hypothesis H_0 that all the considered groups populations come from the same distribution: in other words, the null hypothesis corresponds to the fact that no significant difference is detectable among the groups. The null hypothesis will be accepted or rejected according to a statistical summary $\hat{F}$:

$$\hat{F} = \frac{\frac{\sigma_{bg}^2}{G-1}}{\frac{\sigma_{wg}^2}{N-G}} \simeq F(G-1, N-G), \tag{4}$$

where

$$\sigma_{bg}^2 = \sum_{j=1}^{G} \frac{n_j}{N} \left(\bar{y} - \mu_j\right)^2, \tag{5}$$

$$\sigma_{wg}^2 = \frac{1}{N} \sum_{j=1}^{G} \sum_{i=1}^{n_j} \left(\bar{y}_{ij} - \mu_j\right)^2, \tag{6}$$

with G being the number of groups of size n_j, N being the global number of samples with overall average $\bar{y}$, σ_{bg}^2 being the variance between the groups, σ_{wg}^2 being the variance within the groups (basically the average of the variance computed in each group).

The null hypothesis H_0 will be accepted with a confidence level $1-\alpha$ if the summary $\hat{F}$ is less extreme than a critical value $F^{\alpha}(G-1, N-G)$. The corresponding p-value is computed: it represents the the probability that the summary is more extreme than the observed $\hat{F}$, assuming that H_0 is true. If the p-value is less than α (a typical threshold selection is 5%), H_0 is rejected. These concepts are sketched in Figure 6.

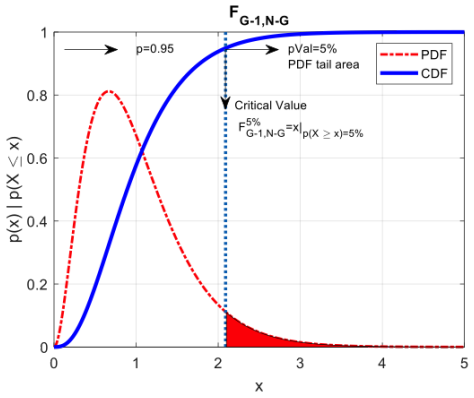

Figure 6: $F(G-1, N-G)$ distribution, with highlighted the 5% critical value and the concept of p-value.

For this analysis, the data sets are divided in 2 groups: the former one contains the healthy samples (TS1-TS6) and the latter one includes the features extracted from the time series of the damaged wind turbine (TS10-18).

3.5 Principal Component Analysis

The PCA [18] is a space rotation to convert a set of correlated quantities into orthogonal variables called principal components: the first principal component explains the largest variance of the data set and each succeeding component explains the largest variance under the constraint of orthogonality with the preceding ones. This technique is widely employed in multivariate statistics and it is powerful for visualizing multi-dimensional data sets by projecting them to the first principal components, i.e. those explaining the largest amount of the variance. In the present study, the statistical features matrix is PCA-rotated and projected to the first principal components, in order to highlight distinguishable features of the damaged wind turbine with respect to the reference ones.

3.6 Novelty Index

The Mahalanobis distance is particularly appropriate for highlighting data discordance in multi-dimensional spaces, because it is non-dimensional and scale-invariant, and takes into account the correlations of the data set. The Mahalanobis distance between one measurement z and the $\boldsymbol{X}$ distribution, whose covariance matrix is $\boldsymbol{S}$, is given by

$$MD = \sqrt{\left(z - \bar{\boldsymbol{X}}\right) \boldsymbol{S}^{-1} \left(z - \bar{\boldsymbol{X}}\right)}. \tag{7}$$

In this study, the reference $\boldsymbol{X}$ distribution is selected as the statistical features matrix extracted from the calibration data set of Table 1 (TS 1-3). The target z is selected as the statistical features matrix extracted from the target data set of interest in Table 1. For example, computing the Mahalanobis distance, according to Equation 7, for each features observation in TS 4-18, it is possible to appreciate the different statistical novelty of the target (healthy, damaged and repaired) wind turbines with respect to the reference healthy ones.

4 Results

The statistical features computed on the cleaned data sets are reported in Figure 7. The vertical lines divide each plot in four areas corresponding respectively to healthy calibration data, healthy validation data, repaired validation data, damaged validation data. From Figure 7, it clearly arise that the damaged wind turbine is clearly distinguishable with respect to the healthy wind turbine and with respect to the repaired wind turbine as well. Some difference arise in the repaired wind turbine with respect to the healthy wind turbines, but it considered not relevant. For this reason, therefore, the data for the hypothesis test are grouped as follows: the ANOVA is performed to test if significant differences can be found between the healthy turbines observations (TS 1 to 9) and the damaged turbines observations (TS 10 to 18) and the results are reported in Table 2. As it can be easily seen, all the features prove to be clearly good for detecting the damage, except the Crest Factor of the accelerations from y-direction channel.

The four data sets (healthy training, healthy validation, repaired validation, damaged validation) are further analyzed via visual inspection in Figure 8. The plots are two-dimensional, in the form of projections of the data set on the first principal components (P1-P2, P1-P3, P2-P3, P3-P4). It can be noticed that the dispersion of the damaged cloud (in red) is much larger, so that the red observations (in particular on the P2-P3 and P3-P4 planes) result more scattered and distinguishable.

Finally, in Figure 9 the Novelty Index (Mahalanobis distance) is reported. The plots is divided by vertical lines similarly to Figure 7, corresponding to healthy calibration data, healthy validation data, repaired validation data, damaged validation data. In red, a threshold is reported for novelty detection based on Montecarlo simulations. It should be noticed that the repaired turbine data seems to show some differences with respect to the original healthy data, but the main novelty detection (consistently with the expectation) regards the damaged wind turbine. In this sense, it can be observed that the Mahalanobis distance is a very responsive metric, because it highlights also some relevant difference between the repaired wind turbine and the healthy wind turbines: these differences do not arise clearly from the qualitative analysis of the statistical features,

also if they are projected to the principal component planes (Figures 7-8). This strongly supports the use of Mahalanobis distance for novelty detection and therefore for early fault diagnosis.

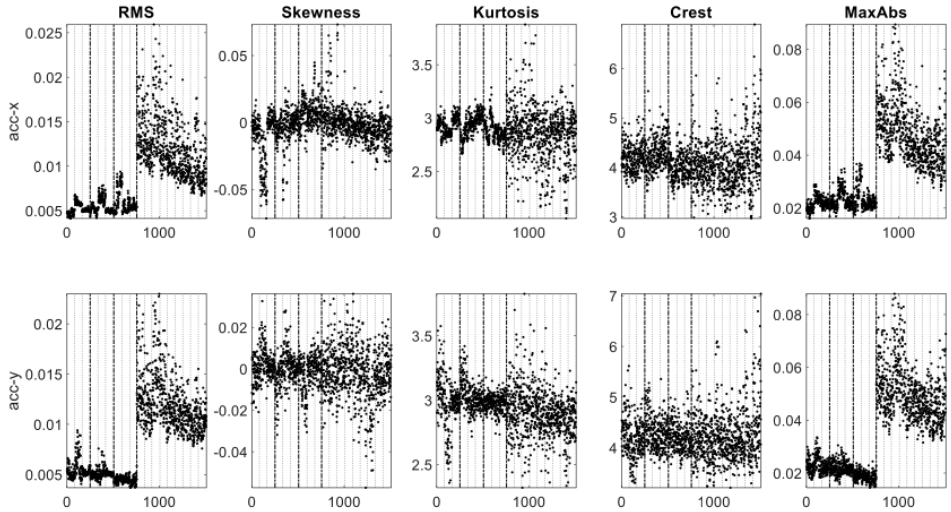

Figure 7: The statistical features computed on the cleaned data set. The different acquisitions are ordered according to their corresponding TS number.

Table 2: The ANOVA p-values considering two groups: Healthy (TS 1 to 9) vs Damaged (TS 10 to 18)

Channel	RMS	Skewness	Kurtosis	Crest Factor	Peak
1 (X-dir)	0	0.28	$1.4 \cdot 10^{-14}$	$8.2 \cdot 10^{-7}$	0
2 (Y-dir)	0	$9.4 \cdot 10^{-7}$	$1.9 \cdot 10^{-35}$	0.59	0

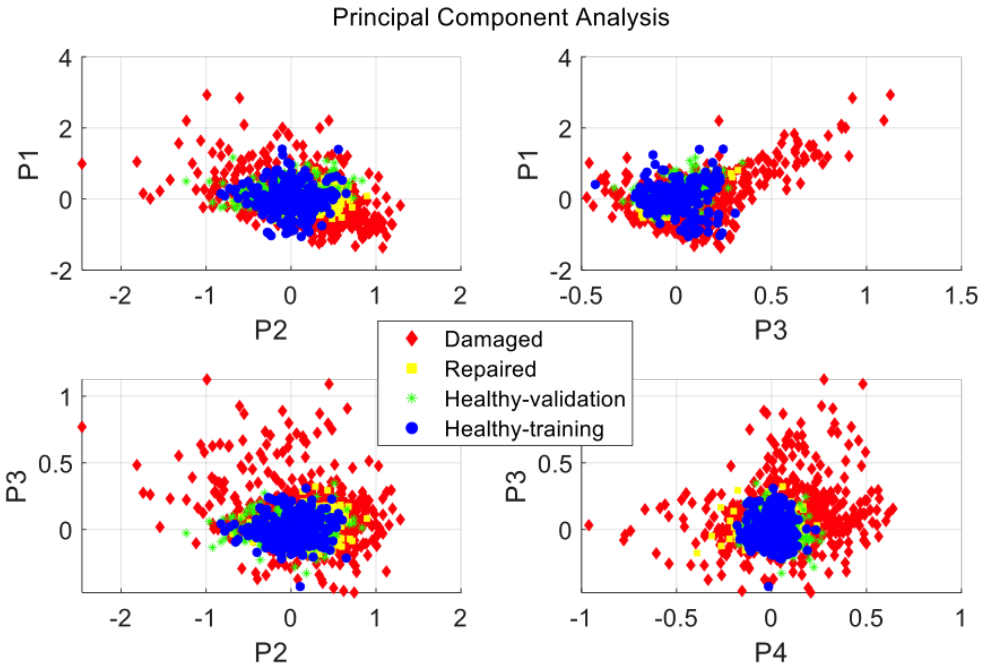

Figure 8: The statistical features computed on the cleaned data set. The different acquisitions are ordered according to their corresponding TS number.

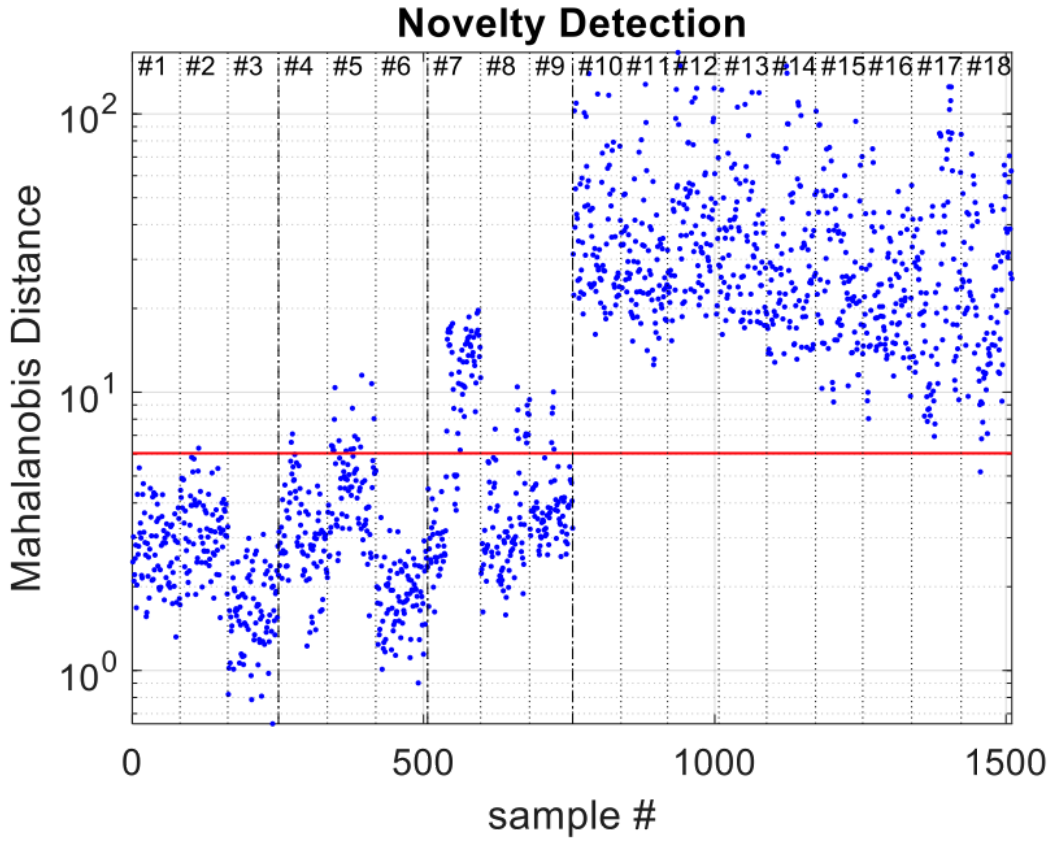

Figure 9: The Novelty Index computed via Mahalanobis Distance.

5 Conclusions

This study has been devoted to the investigation of the possibility of reliably diagnosing wind turbine drivetrain damages through the analysis of vibrations measured at the tower. The rationale for inquiring this possibility is the perspective of setting up an unsupervised condition monitoring approach that can be employed on a large scale, without intervening on wind turbines operation. There are studies [10] supporting that this objective is achievable, basing on the analysis of the correlation between tower vibrations and vibrations collected at a damaged generator bearing. The objective of this study has been renouncing to the crosscheck against vibrations at the target sub-components: the keystone has been comparing the wind turbines at the same wind farm, by measuring consecutively or almost consecutively at the highest possible number of wind turbines. The problem therefore translates in highlighting the distinguishable features of the tower vibrations at the damaged wind turbine with respect to the reference undamaged wind turbines.

A test case has been discussed in this work: it is a wind farm featuring six 2 MW wind turbines, one of which had a damage at the high speed shaft bearing when the measurements were collected. Three reference healthy wind turbines have been selected and a further target wind turbines has been individuated because it suffered a planetary bearing damage and was recovered when the measurements have been collected.

The collected data have been appropriately pre-processed and statistical features (root mean square, skewness, kurtosis, peak, crest factor) have been computed on independent excerpts of the time series. Through Univariate Analysis of Variance, Principal Component Analysis, Novelty Analysis through the Mahalanobis distance it has been possible to clearly distinguish the damaged wind turbine, while the recovered wind turbine resulted being substantially indistinguishable with respect to the healthy reference wind turbines.

In general, the algorithm proved to be an excellent damage detection routine, considering the quickness, the simplicity and the full independence from human interaction, which makes it suitable for real time implementations. Another important development of this research is empowering the experimental techniques, in order to have high-frequency rotor angular speed measurements: this direction is currently being explored through video-tachometer [19] because it preserves the zero-impact philosophy of the approach. The availability of this kind of information, as well as of the gearbox geometry, is decisive for obtaining a precise identification of the damage location.

A further direction is being explored and it has been inspired by the impossibility of performing on site measurement during the period of COVID-19 outbreak: it deals with this kind of analysis applied on the data provided by the industrial condition monitoring system of the wind turbines, where available.

Acknowledgements

The authors would like to thank Ludovico Terzi, technology manager of the Renvico company. The authors acknowledge Fondazione “Cassa di Risparmio di Perugia” for the funded research project WIND4EV (WIND turbine technology EVolution FOR lifecycle optimization).

References

[1] J. Rafiee, F. Arvani, A. Harifi, and M. Sadeghi, “Intelligent condition monitoring of a gearbox using artificial neural network,” *Mechanical systems and signal processing*, vol. 21, no. 4, pp. 1746–1754, 2007.

[2] T. Wang, Q. Han, F. Chu, and Z. Feng, “Vibration based condition monitoring and fault diagnosis of wind turbine planetary gearbox: A review,” *Mechanical Systems and Signal Processing*, vol. 126, pp. 662–685, 2019.

[3] F. Spinato, P. J. Tavner, G. J. Van Bussel, and E. Koutoulakos, “Reliability of wind turbine subassemblies,” *IET Renewable Power Generation*, vol. 3, no. 4, pp. 387–401, 2009.

[4] P. Tavner, F. Spinato, G. Van Bussel, and E. Koutoulakos, "Reliability of different wind turbine concepts with relevance to offshore application," in *European Wind Energy Conference*, 2008.

[5] H. D. M. de Azevedo, A. M. Araújo, and N. Bouchonneau, "A review of wind turbine bearing condition monitoring: State of the art and challenges," *Renewable and Sustainable Energy Reviews*, vol. 56, pp. 368–379, 2016.

[6] J. Antoni, "Cyclic spectral analysis in practice," *Mechanical Systems and Signal Processing*, vol. 21, no. 2, pp. 597–630, 2007.

[7] Z. Feng, X. Chen, and M. Liang, "Iterative generalized synchrosqueezing transform for fault diagnosis of wind turbine planetary gearbox under nonstationary conditions," *Mechanical Systems and Signal Processing*, vol. 52, pp. 360–375, 2015.

[8] X. Wang, X. Yan, and Y. He, "Weak fault feature extraction and enhancement of wind turbine bearing based on ocycbd and svdd," *Applied Sciences*, vol. 9, no. 18, p. 3706, 2019.

[9] M. Elforjani, "Diagnosis and prognosis of real world wind turbine gears," *Renewable Energy*, vol. 147, pp. 1676–1693, 2020.

[10] E. Mollasalehi, D. Wood, and Q. Sun, "Indicative fault diagnosis of wind turbine generator bearings using tower sound and vibration," *Energies*, vol. 10, no. 11, p. 1853, 2017.

[11] F. Castellani, L. Garibaldi, A. P. Daga, D. Astolfi, and F. Natili, "Diagnosis of faulty wind turbine bearings using tower vibration measurements," *Energies*, vol. 13, no. 6, p. 1474, 2020.

[12] A. P. Daga and L. Garibaldi, "Machine vibration monitoring for diagnostics through hypothesis testing," *Information*, vol. 10, no. 6, p. 204, 2019.

[13] S. W. Smith *et al.*, "The scientist and engineer's guide to digital signal processing," 1997.

[14] H. Liu, S. Shah, and W. Jiang, "On-line outlier detection and data cleaning," *Computers & chemical engineering*, vol. 28, no. 9, pp. 1635–1647, 2004.

[15] R. K. Pearson, Y. Neuvo, J. Astola, and M. Gabbouj, "The class of generalized hampel filters," in *2015 23rd European Signal Processing Conference (EUSIPCO)*. IEEE, 2015, pp. 2501–2505.

[16] A. P. Daga, A. Fasana, S. Marchesiello, and L. Garibaldi, "The politecnico di torino rolling bearing test rig: Description and analysis of open access data," *Mechanical Systems and Signal Processing*, vol. 120, pp. 252–273, 2019.

[17] M. Hubert and M. Debruyne, "Minimum covariance determinant," *Wiley interdisciplinary reviews: Computational statistics*, vol. 2, no. 1, pp. 36–43, 2010.

[18] H. Abdi and L. J. Williams, "Principal component analysis," *Wiley interdisciplinary reviews: computational statistics*, vol. 2, no. 4, pp. 433–459, 2010.

[19] A. P. Daga and L. Garibaldi, "Ga-adaptive template matching for offline shape motion tracking based on edge detection: Ias estimation from the survishno 2019 challenge video for machine diagnostics purposes," *Algorithms*, vol. 13, no. 2, p. 33, 2020.